New Journal of Chemistry

Synthesis and optoelectronic properties of spirofluorenexanthene-based carbazole host materials

Supporting Information

Mingli Sun [a], Shouzhen Yue [b], Changjin Ou [c], Baoyi Ren [d,*], Yan Qian [c], Yi Zhao [b], Linghai Xie [c], and Wei Huang [c]

Characterization

^{1}H-NMR in $CDCl_3$ was recorded at 400 MHz using a Varian Mercury 400 plus spectrometer. For the MALDI-TOF MS(Bruker Daltonics, Germany) spectra, the spectra were recorded in reflective mode, no substrates were used. Absorption spectra were measured with a Shimadzu UV-3600 spectrometer and emission spectra were recorded on a Shimadzu RF-5301PC luminescence spectrometer. Thermogravimetric analyses (TGA) were conducted on a Shimadzu DTG-60H thermogravimetric Analyzer under a heating rate of 10°C/min and a nitrogen flow rate of 20 cm^3/min. Cyclic voltammetric (CV) studies were conducted using an CHI600C in a typical three-electrode cell with a platinum sheet working electrode, a platinum wire counter electrode, and a silver/silver nitrate (Ag/Ag^+) reference electrode.

Notes and references

[a]*College of Chemistry, Chemical Engineering and Resource Utilization, Northeast Forestry University, 26 Hexing Road, Harbin 150040, China*

[b]*State Key Laboratory on Integrated Optoelectronics, College of Electronic Science and Engineering, Jilin University, 2699 Qianjin Street, Changchun 130013, China*

[c]*Key Laboratory for Organic Electronics and Information Displays & Jiangsu Key Laboratory for Biosensors, Institute of Advanced Materials (IAM), Jiangsu National Synergistic Innovation Center for Advanced Materials (SICAM), Nanjing University of Posts & Telecommunications, 9 Wenyuan Road, Nanjing 210023, China*

[d]*College of Science, Shenyang University of Chemical Technology, No. 11 Street, Shenyang Economic and Technological Development Area, Shenyang 110142, China*

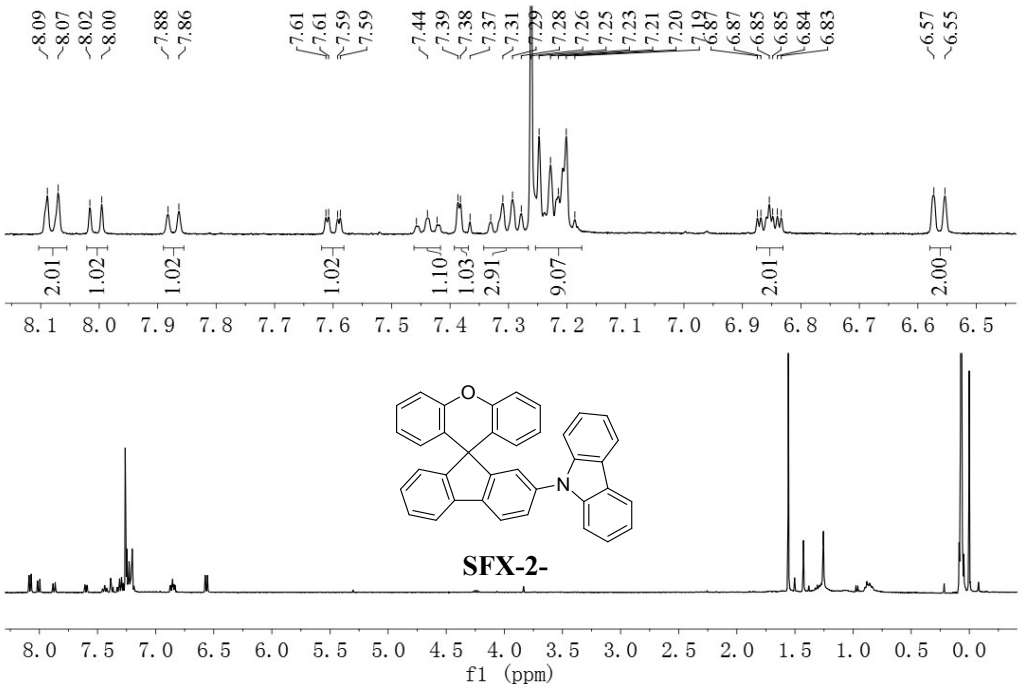

Figure S1. ^{1}H-NMR of SFX-2-Cz.

^{1}H NMR (400 MHz, $CDCl_3$) δ 8.08 (d, *J* = 7.4 Hz, 2H), 8.01 (d, *J* = 8.1 Hz, 1H), 7.87 (d, *J* = 7.4 Hz, 1H), 7.60 (dd, *J* = 8.0, 1.8 Hz, 1H), 7.44 (t, *J* = 7.1 Hz, 1H), 7.38 (d, *J* = 1.7 Hz, 1H), 7.30 (dd, *J* = 13.8, 7.1 Hz, 3H), 7.25 – 7.17 (m, 9H), 6.88 – 6.83 (m, 2H), 6.56 (d, *J* = 7.6 Hz, 2H).

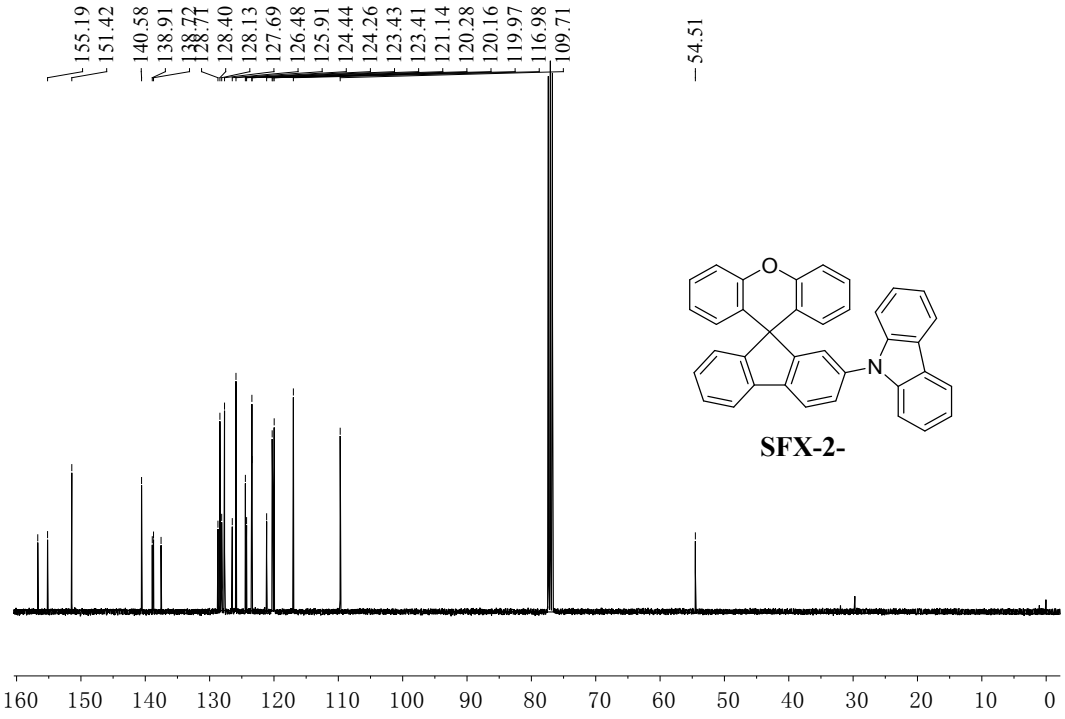

Figure S2. ^{13}C-NMR of SFX-2-Cz.

^{13}C NMR (101 MHz, $CDCl_3$) δ 156.71 (s), 155.19 (s), 151.42 (s), 140.58 (s), 138.82 (d, *J* = 19.5 Hz), 137.55 (s), 128.71 (s), 128.40 (s), 128.13 (s), 127.69 (s), 126.48 (s), 125.91 (s), 124.35 (d, *J* = 18.6 Hz), 123.42 (d, *J* = 2.5 Hz), 121.14 (s), 120.38 – 119.87 (m), 116.98 (s), 109.71 (s), 54.51 (s).

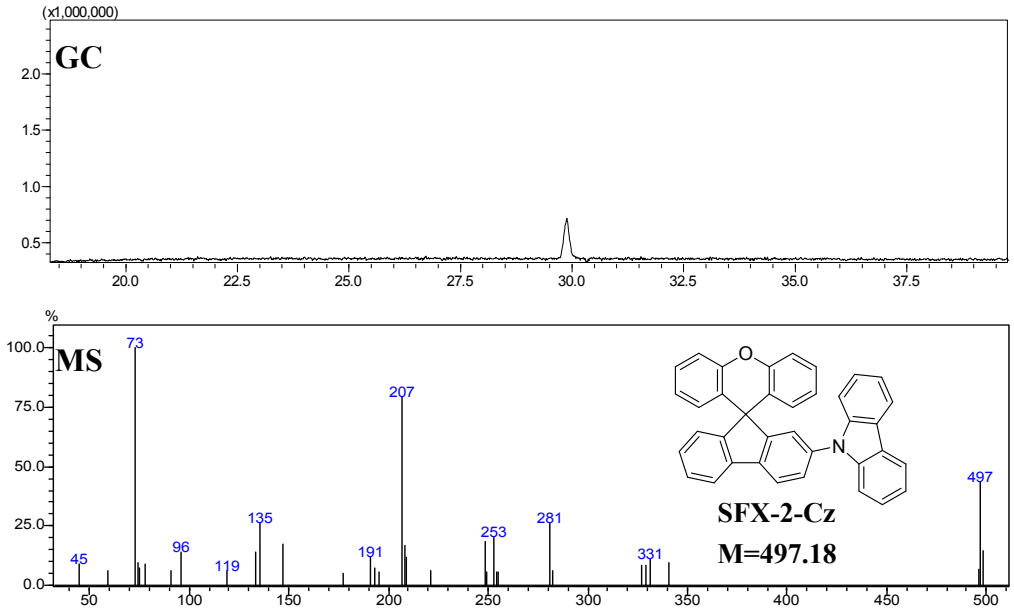

Figure S3. GC-MS of SFX-2-Cz

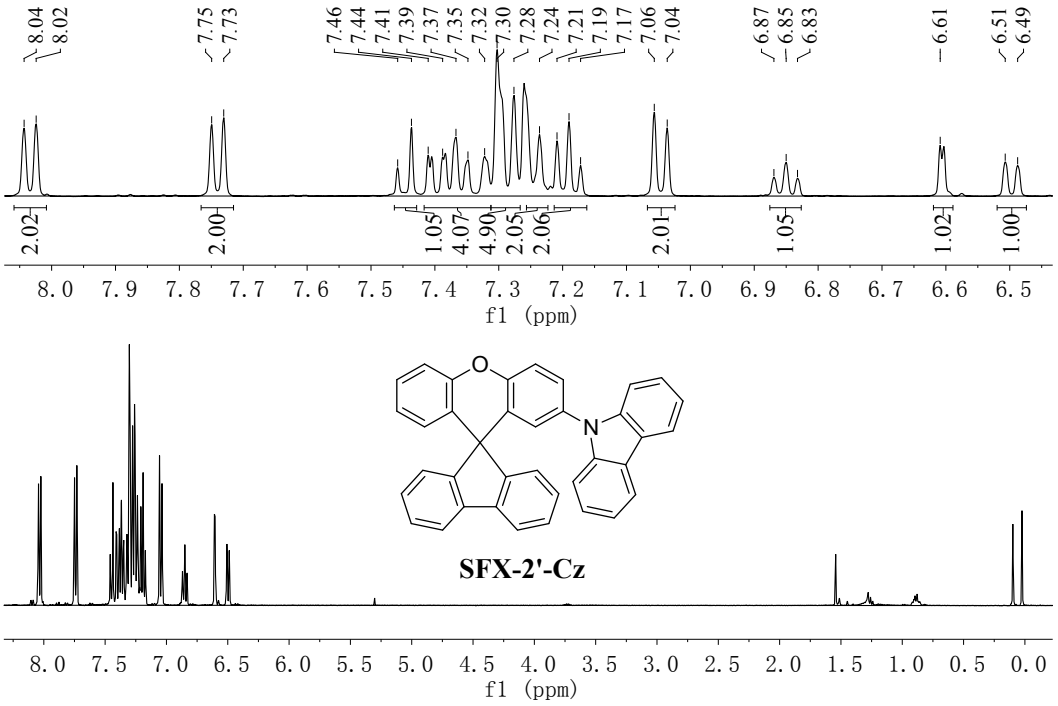

Figure S4. ^{1}H-NMR of SFX-2'-Cz.

^{1}H NMR (400 MHz, $CDCl_3$) δ 8.03 (d, J = 7.6 Hz, 2H), 7.74 (d, J = 7.6 Hz, 2H), 7.45 (d, J = 8.6 Hz, 1H), 7.42 – 7.31 (m, 4H), 7.29 (d, J = 10.6 Hz, 5H), 7.24 (s, 2H), 7.19 (t, J = 7.4 Hz, 2H), 7.05 (d, J = 8.1 Hz, 2H), 6.85 (t, J = 7.4 Hz, 1H), 6.61 (s, 1H), 6.50 (d, J = 7.8 Hz, 1H).

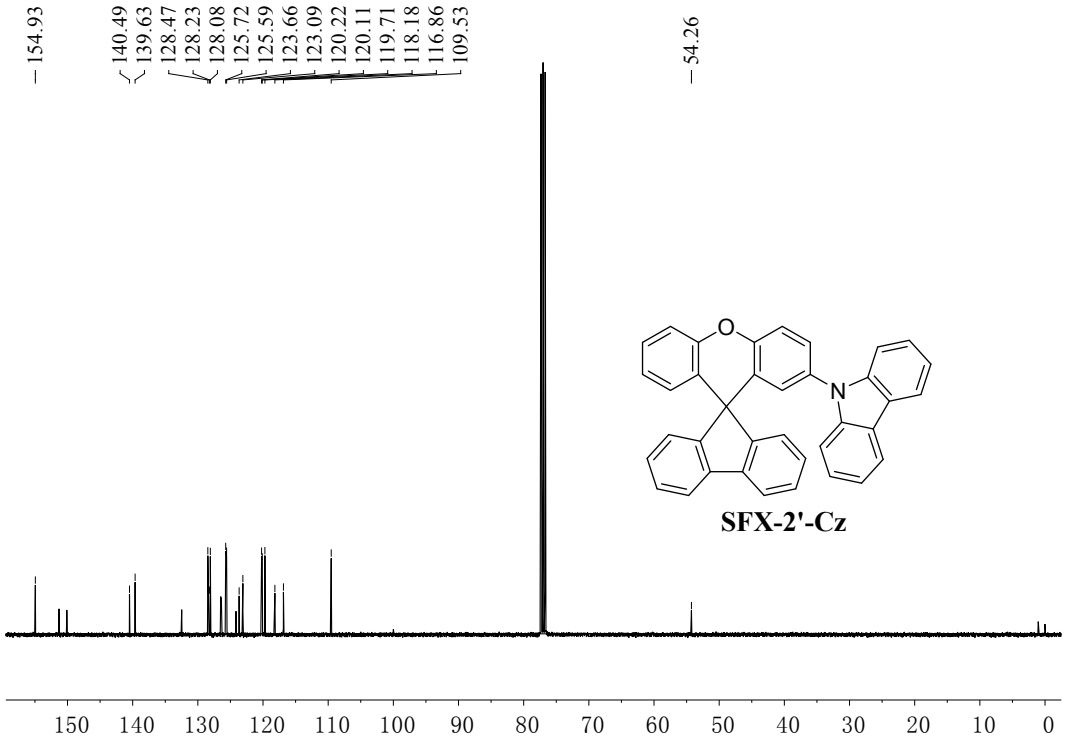

Figure S5. ^{13}C-NMR of SFX-2'-Cz

^{13}C NMR (101 MHz, $CDCl_3$) δ 154.93 (s), 140.49 (s), 139.63 (s), 128.47 (s), 128.15 (d, J = 14.5 Hz), 125.65 (d, J = 13.7 Hz), 123.66 (s), 123.09 (s), 120.17 (d, J = 10.3 Hz), 119.71 (s), 118.18 (s), 116.86 (s), 109.53 (s), 54.26 (s).

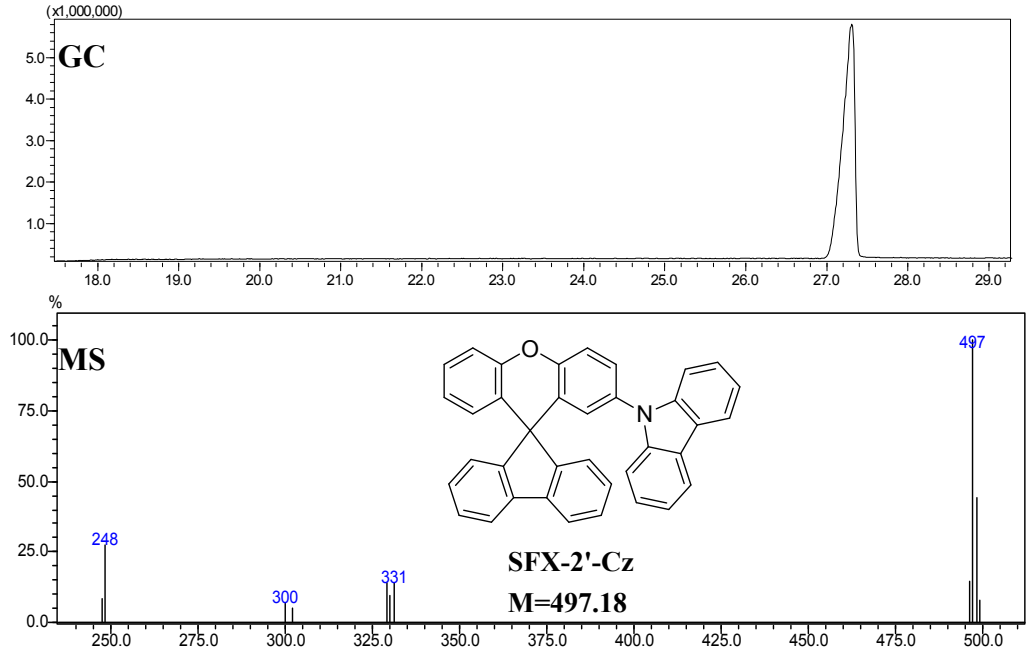

Figure S6. GC-MS of SFX-2'-Cz

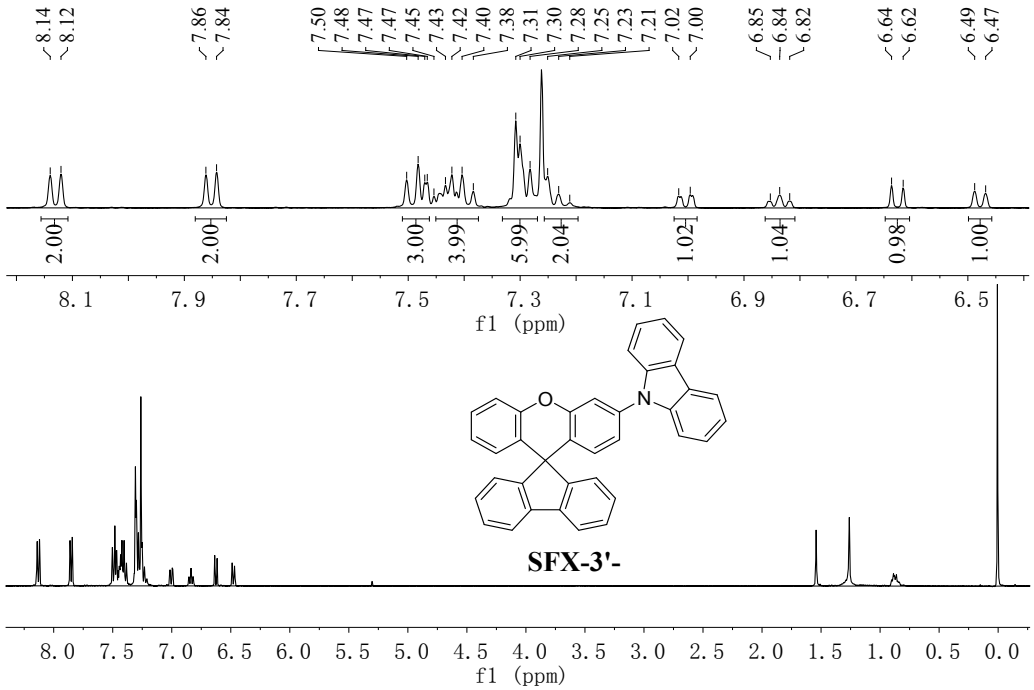

Figure S7. ^{1}H-NMR of SFX-3'-Cz.

^{1}H NMR (400 MHz, $CDCl_3$) δ 8.13 (d, *J* = 7.7 Hz, 2H), 7.85 (d, *J* = 7.6 Hz, 2H), 7.48 (dd, *J* = 9.7, 5.0 Hz, 3H), 7.41 (dd, *J* = 13.6, 6.3 Hz, 4H), 7.33 – 7.27 (m, 6H), 7.26 – 7.20 (m, 2H), 7.01 (d, *J* = 8.2 Hz, 1H), 6.84 (t, *J* = 6.9 Hz, 1H), 6.63 (d, *J* = 8.3 Hz, 1H), 6.48 (d, *J* = 7.9 Hz, 1H).

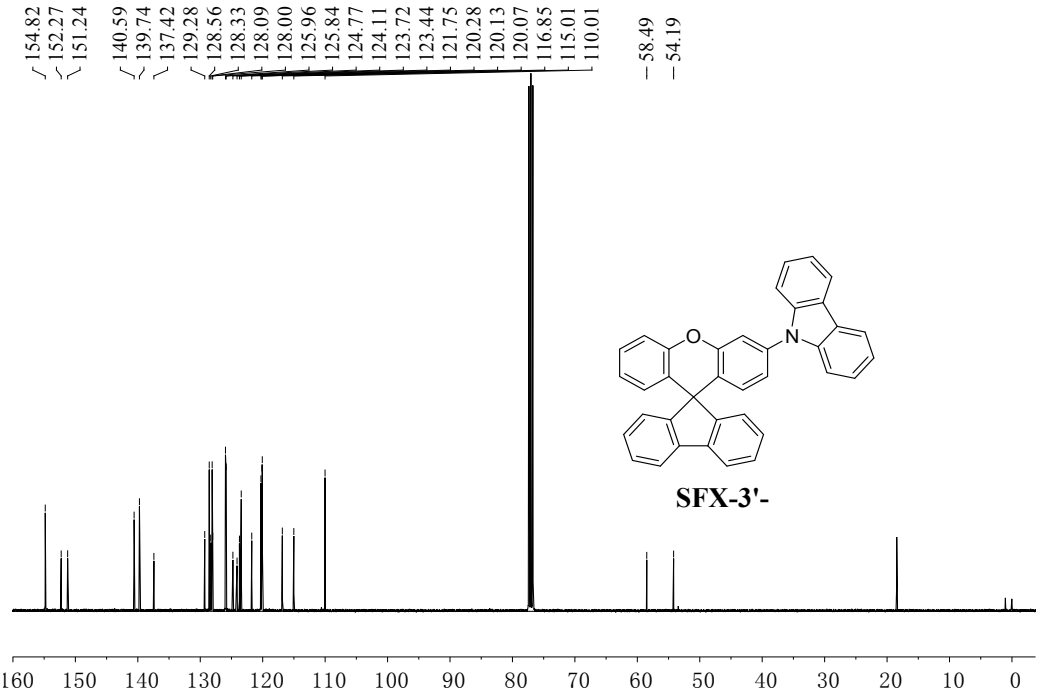

Figure S8. ^{13}C-NMR of SFX-3'-Cz

^{13}C NMR (101 MHz, $CDCl_3$) δ 154.82 (s), 152.27 (s), 151.24 (s), 140.59 (s), 139.74 (s), 137.42 (s), 129.28 (s), 128.56 (s), 128.33 (s), 128.05 (d, *J* = 8.9 Hz), 125.90 (d, *J* = 12.2 Hz), 124.77 (s), 124.11 (s), 123.72 (s), 123.44 (s), 121.75 (s), 120.38 – 119.97 (m), 116.85 (s), 115.01 (s), 110.01 (s), 58.49 (s), 54.19 (s).

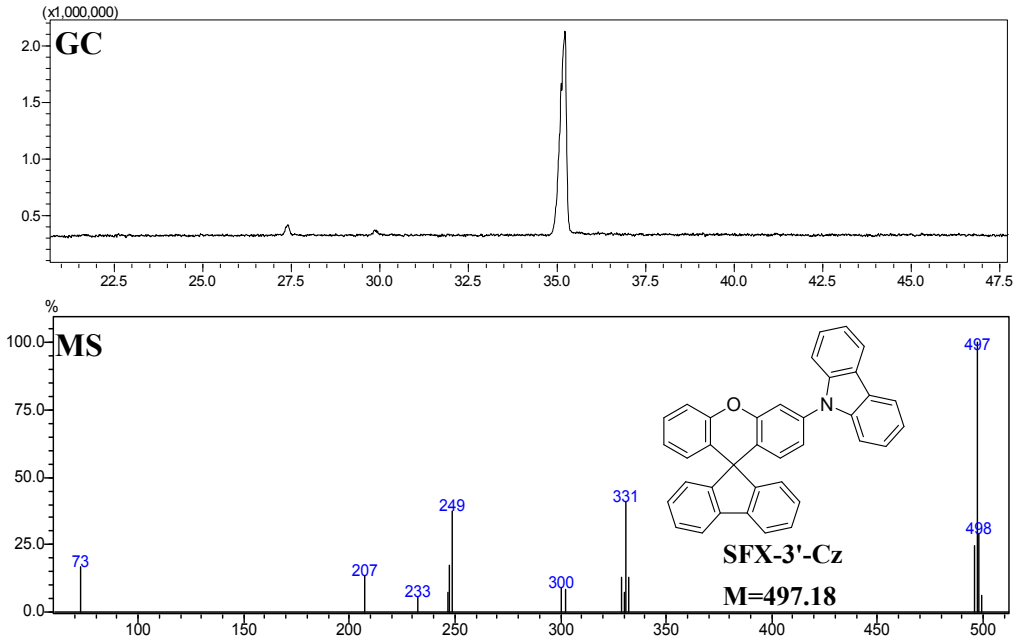

Figure S9. GC-MS of SFX-3'-Cz

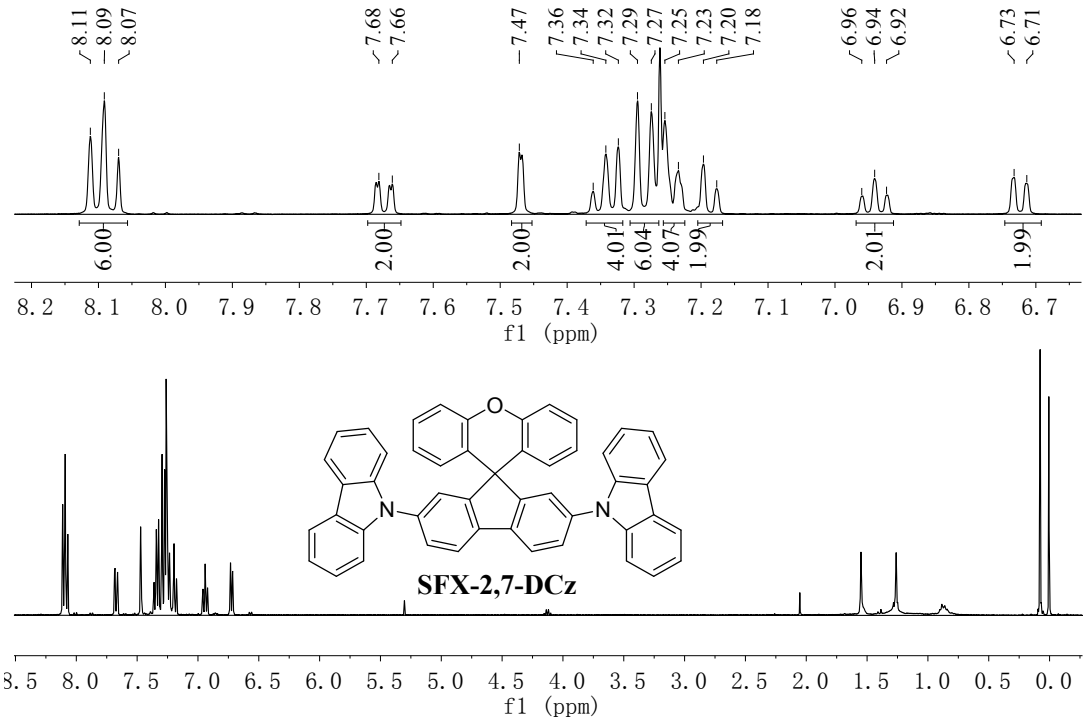

Figure S10. ^{1}H-NMR of SFX-2,7-DCz

^{1}H NMR (400 MHz, $CDCl_3$) δ 8.09 (t, J = 8.4 Hz, 6H), 7.67 (d, J = 8.0 Hz, 2H), 7.47 (s, 2H), 7.37 – 7.32 (m, 4H), 7.28 (d, J = 8.3 Hz, 6H), 7.24 (d, J = 8.1 Hz, 4H), 7.19 (d, J = 7.9 Hz, 2H), 6.94 (t, J = 7.4 Hz, 2H), 6.72 (d, J = 7.6 Hz, 2H).

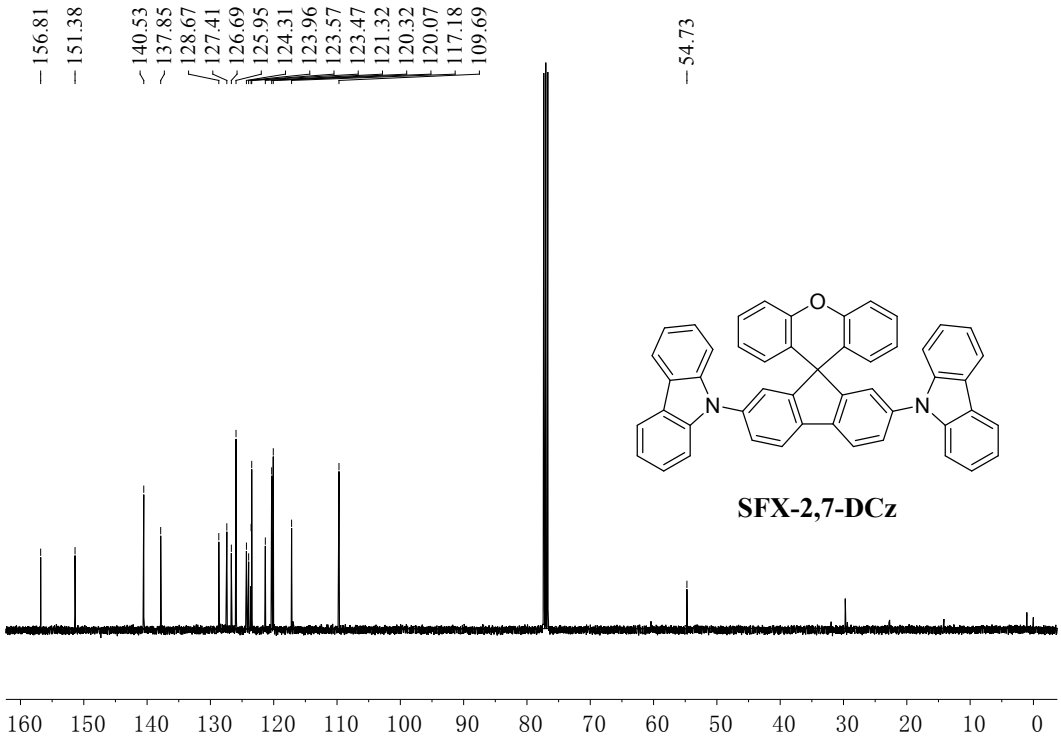

Figure S11. ^{13}C-NMR of SFX-2,7-DCz

^{13}C NMR (101 MHz, $CDCl_3$) δ 156.81 (s), 151.38 (s), 140.53 (s), 137.85 (s), 128.67 (s), 127.41 (s), 126.69 (s), 125.95 (s), 124.31 (s), 123.96 (s), 123.52 (d, J = 10.1 Hz), 121.32 (s), 120.32 (s), 120.07 (s), 117.18 (s), 109.69 (s), 54.73 (s).

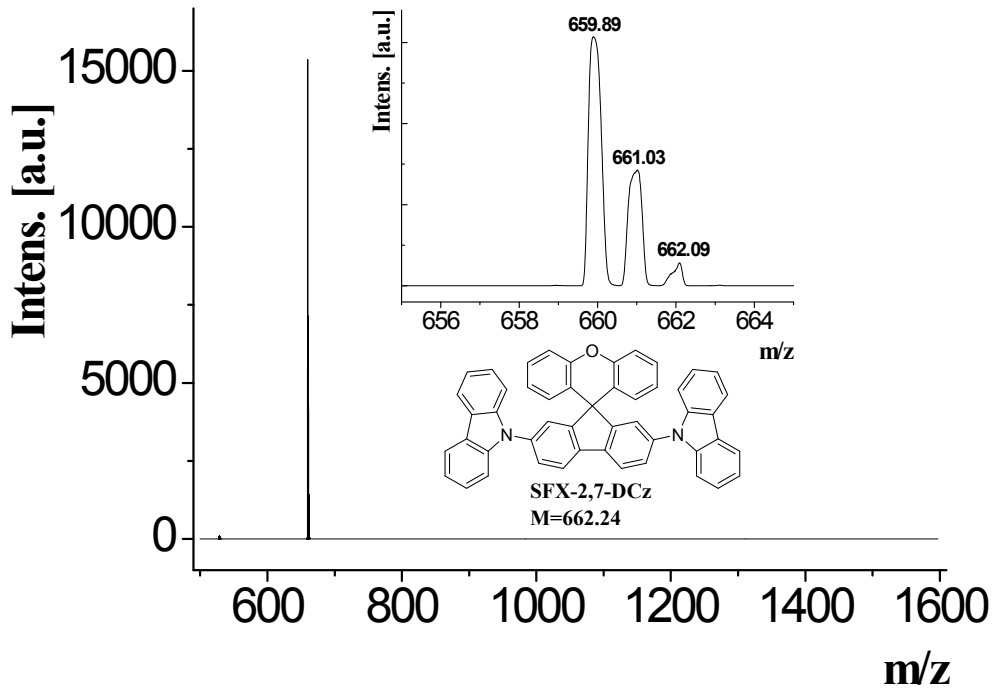

Figure S12. MALDI-TOF-MS of SFX-2,7-DCz

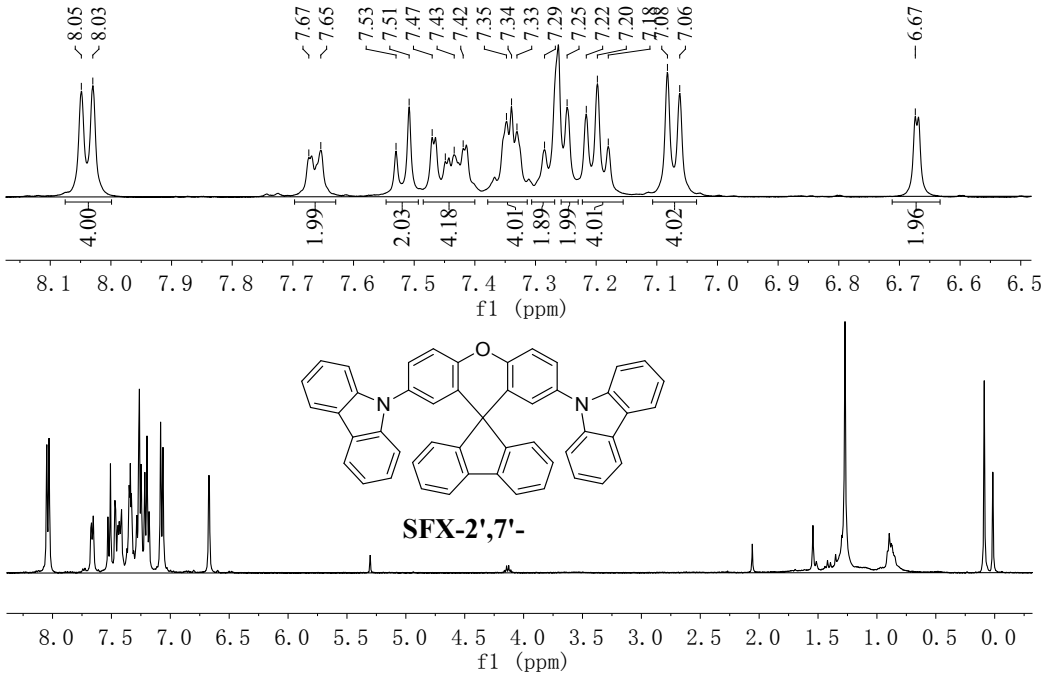

Figure S13. ^{1}H-NMR of SFX-2',7'-DCz

^{1}H NMR (400 MHz, $CDCl_3$) δ 8.04 (d, *J* = 7.6 Hz, 4H), 7.66 (d, *J* = 7.9 Hz, 2H), 7.52 (d, *J* = 8.7 Hz, 2H), 7.44 (dd, *J* = 13.2, 7.3 Hz, 4H), 7.38 – 7.31 (m, 4H), 7.29 (s, 2H), 7.25 (s, 2H), 7.20 (t, *J* = 7.3 Hz, 4H), 7.07 (d, *J* = 8.1 Hz, 4H), 6.67 (s, 2H).

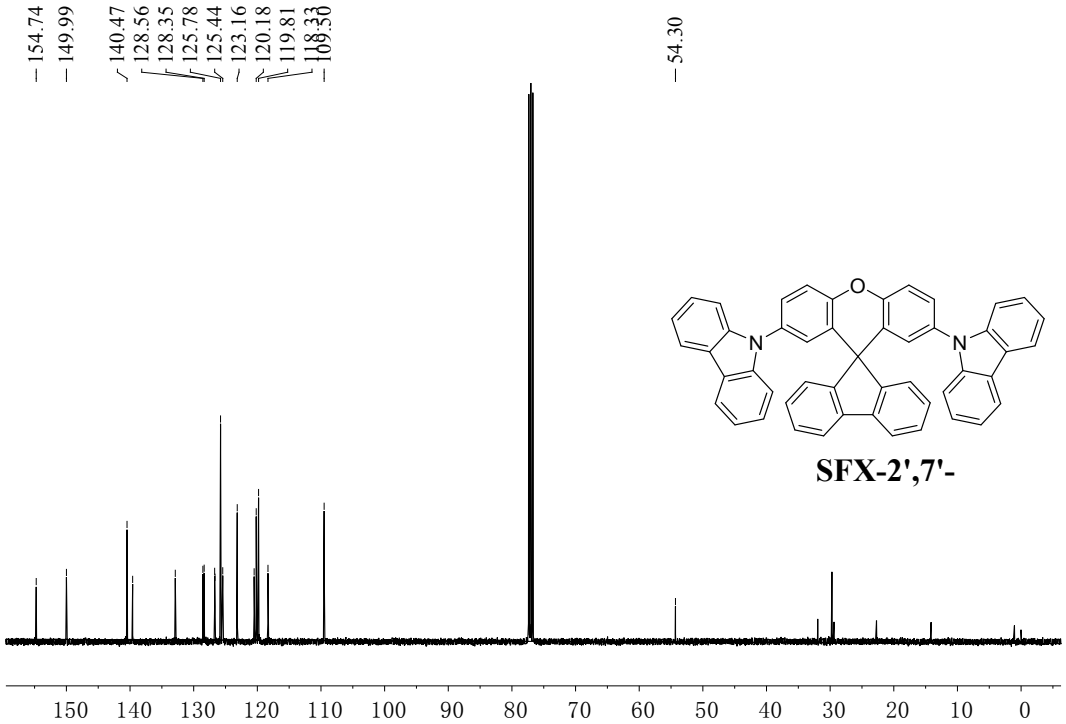

Figure S14. ^{13}C-NMR of SFX-2',7'-DCz

^{13}C NMR (101 MHz, $CDCl_3$) δ 154.74 (s), 149.99 (s), 140.47 (s), 139.59 (s), 132.89 (s), 128.56 (s), 128.35 (s), 126.68 (d, *J* = 5.4 Hz), 125.78 (s), 125.44 (s), 123.16 (s), 120.50 (s), 120.18 (s), 119.81 (s), 118.33 (s), 109.50 (s), 54.30 (s).

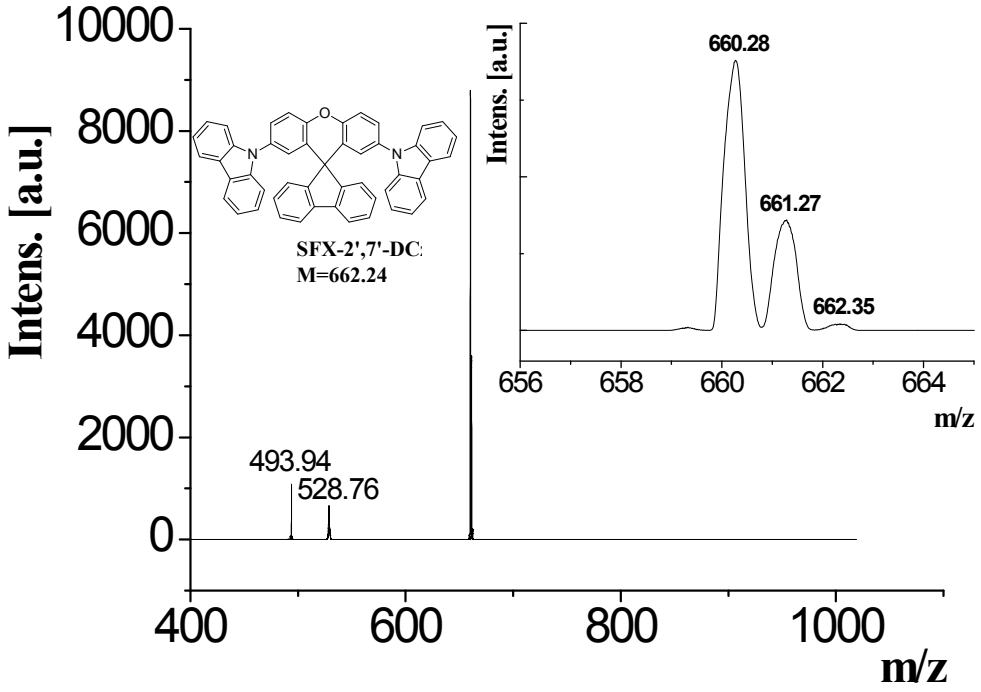

Figure S15. MALDI-TOF-MS of SFX-2',7'-DCz

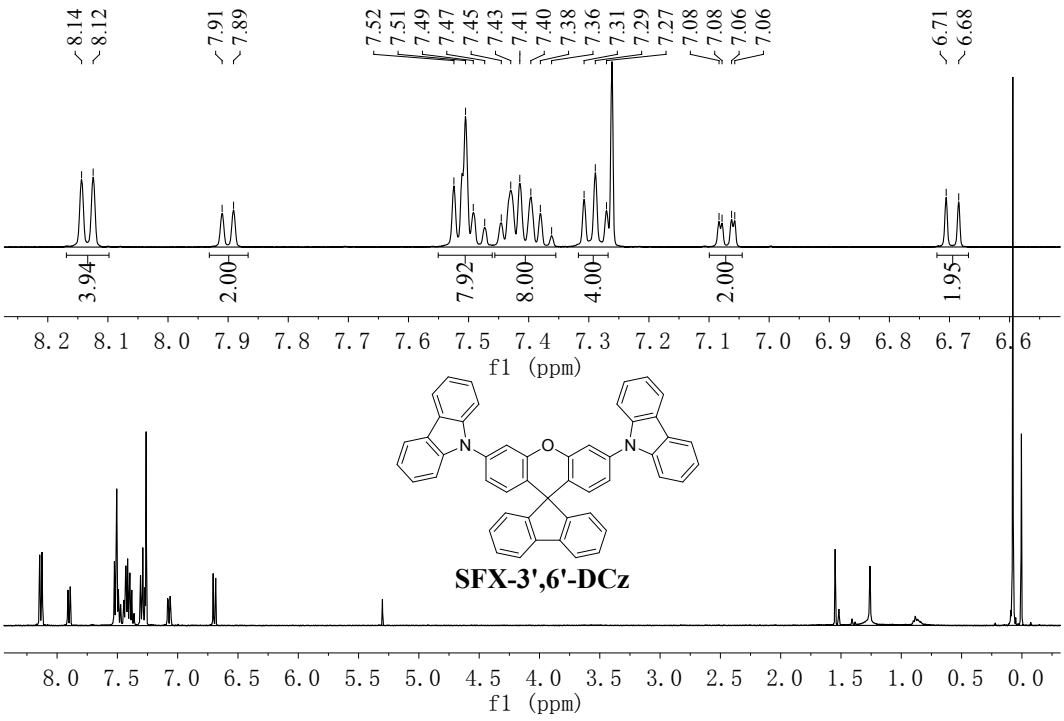

Figure S16. ^{1}H-NMR of SFX-3',6'-DCz

^{1}H NMR (400 MHz, $CDCl_3$) δ 8.13 (d, J = 7.7 Hz, 4H), 7.90 (d, J = 7.6 Hz, 2H), 7.50 (dd, J = 12.8, 7.7 Hz, 8H), 7.46 – 7.35 (m, 8H), 7.29 (t, J = 7.5 Hz, 4H), 7.07 (dd, J = 8.4, 2.1 Hz, 2H), 6.70 (d, J = 8.3 Hz, 2H).

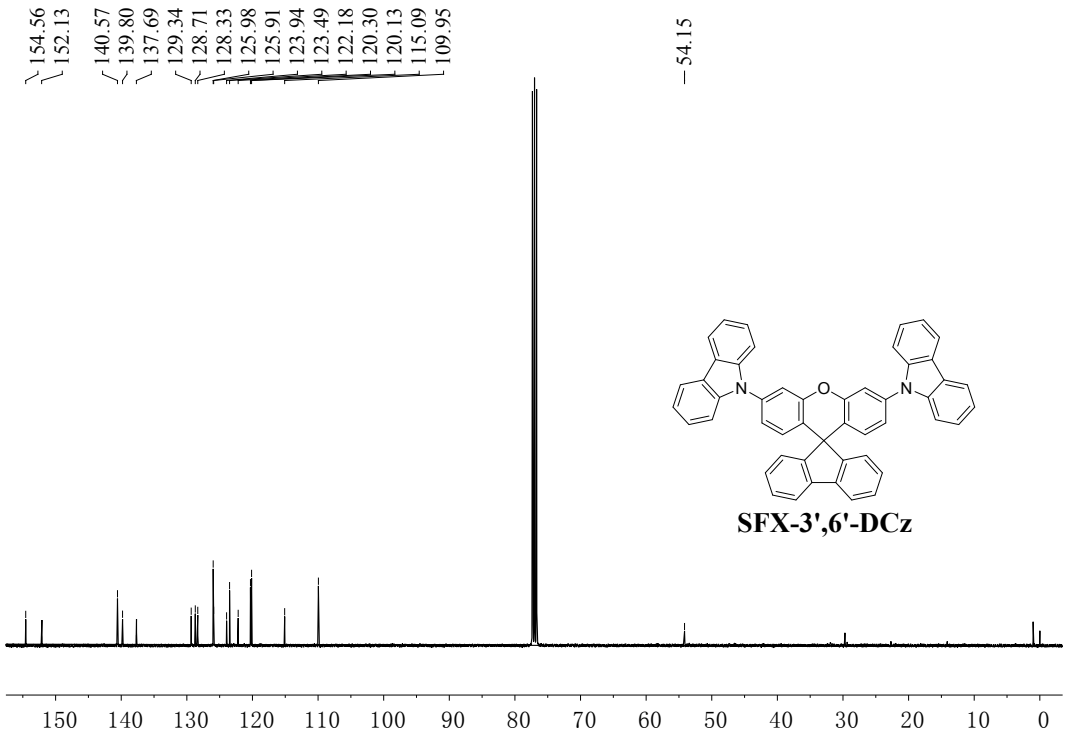

Figure S17. ^{13}C-NMR of SFX-3',6'-DCz

^{13}C NMR (101 MHz, $CDCl_3$) δ 154.56 (s), 152.13 (s), 140.57 (s), 139.80 (s), 137.69 (s), 129.34 (s), 128.71 (s), 128.33 (s), 125.95 (d, J = 7.5 Hz), 123.94 (s), 123.49 (s), 122.18 (s), 120.22 (d, J = 17.1 Hz), 115.09 (s), 109.95 (s), 54.15 (s).

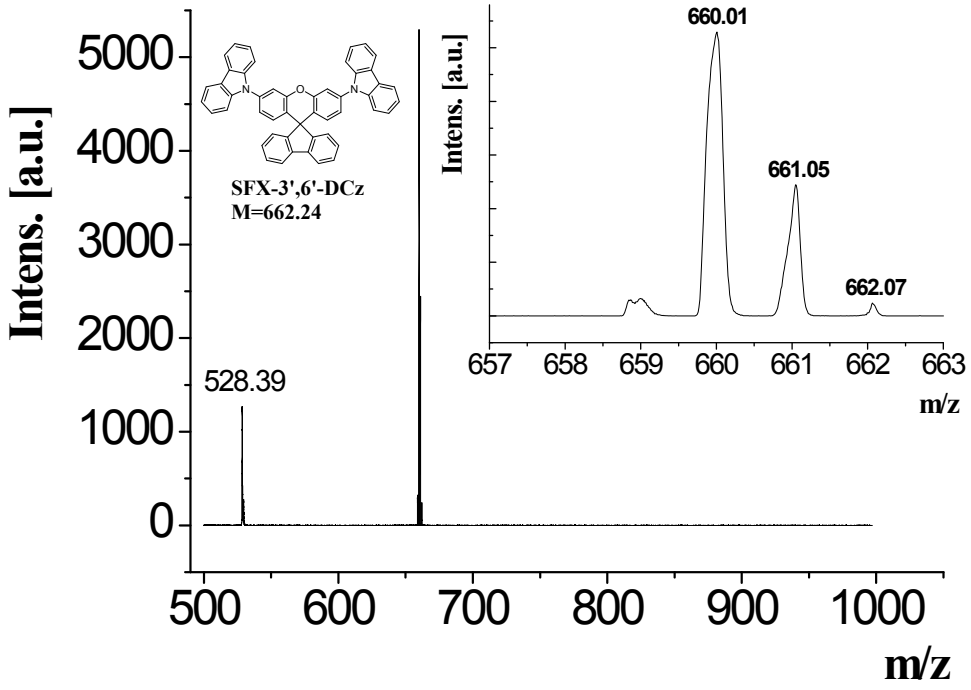

Figure S18. MALDI-TOF-MS of SFX-3',6'-DCz

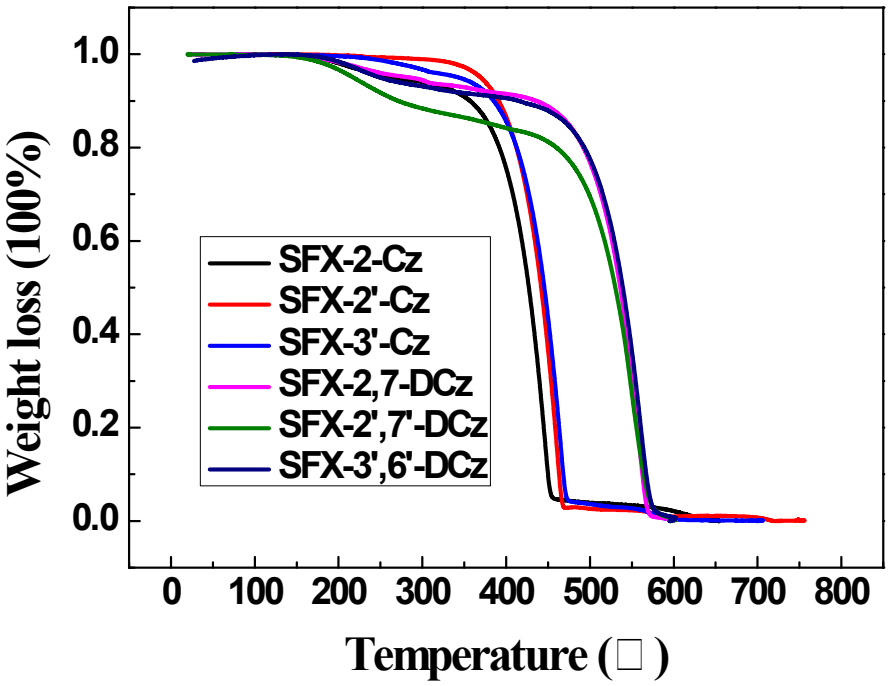

Figure S19. TGA curves of SFX-Cz derivatives recorded at a heating rate of 5 ˚C/min.

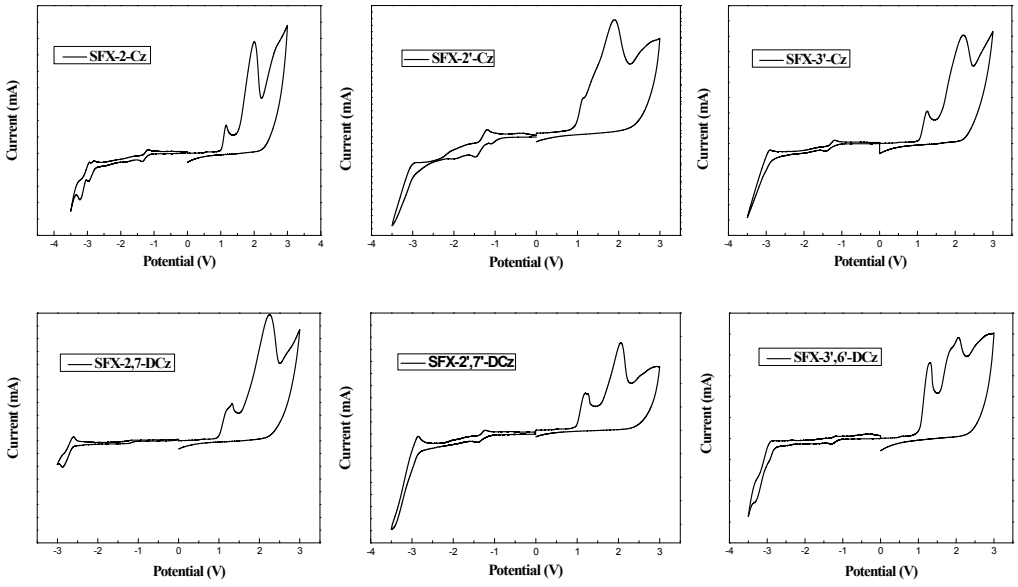

Figure S20. Cyclic voltammograms of SFX-Cz derivatives (reduction in THF solution and oxidation in CH_2Cl_2 solution).

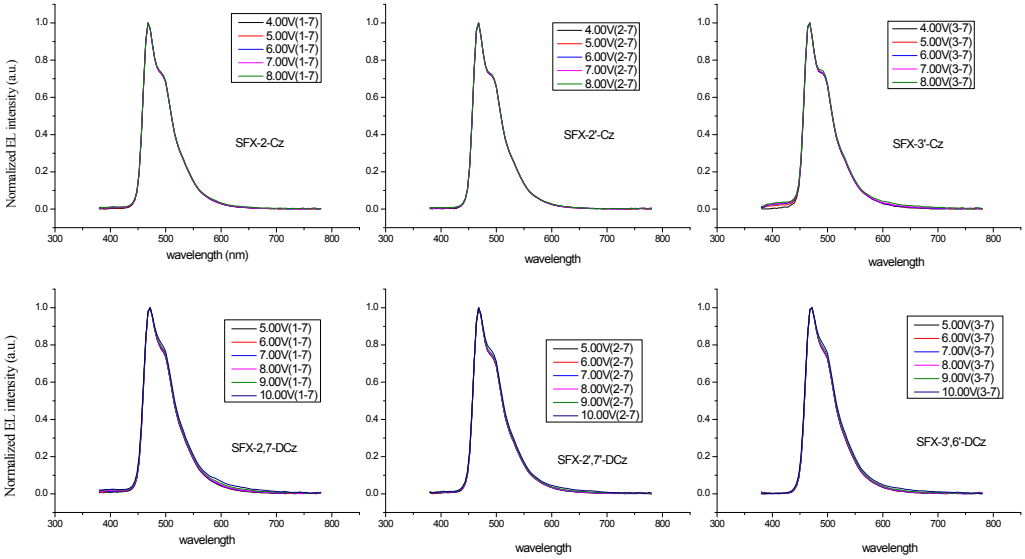

Figure S21. EL spectra of blue-emitting devices based on SFX-Cz hosts.

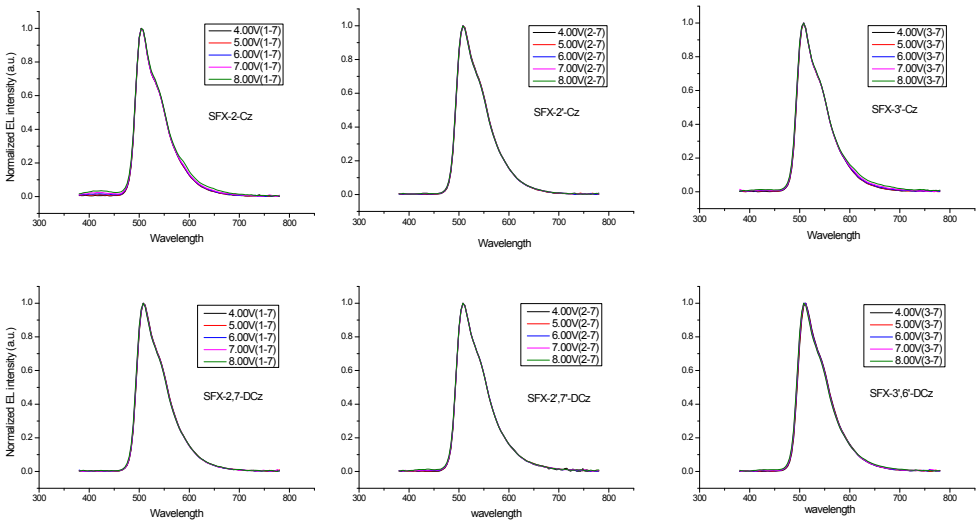

Figure S22. EL spectra of green-emitting devices based on SFX-Cz hosts.

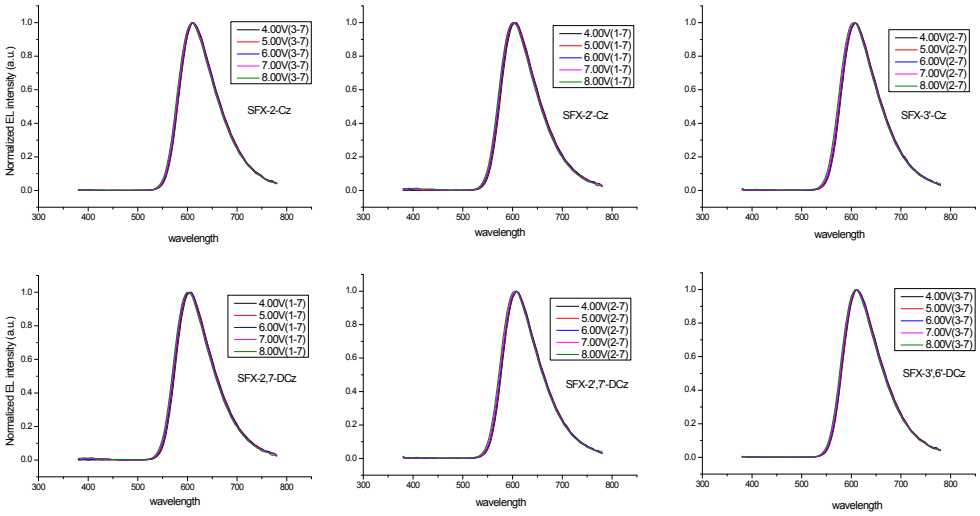

Figure S23. EL spectra of red-emitting devices based on SFX-Cz hosts.

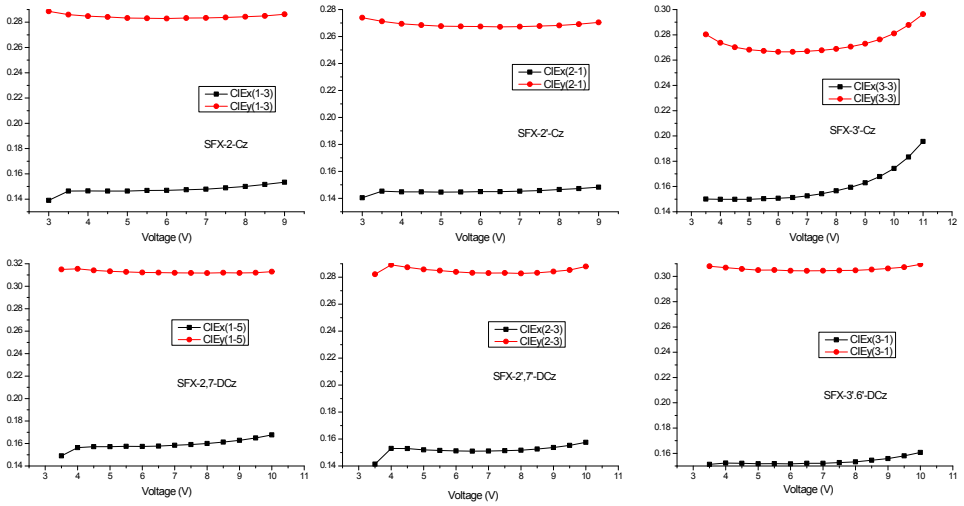

Figure S24. The CIE coordinates versus the voltage of the blue devices based on SFX-Cz hosts.

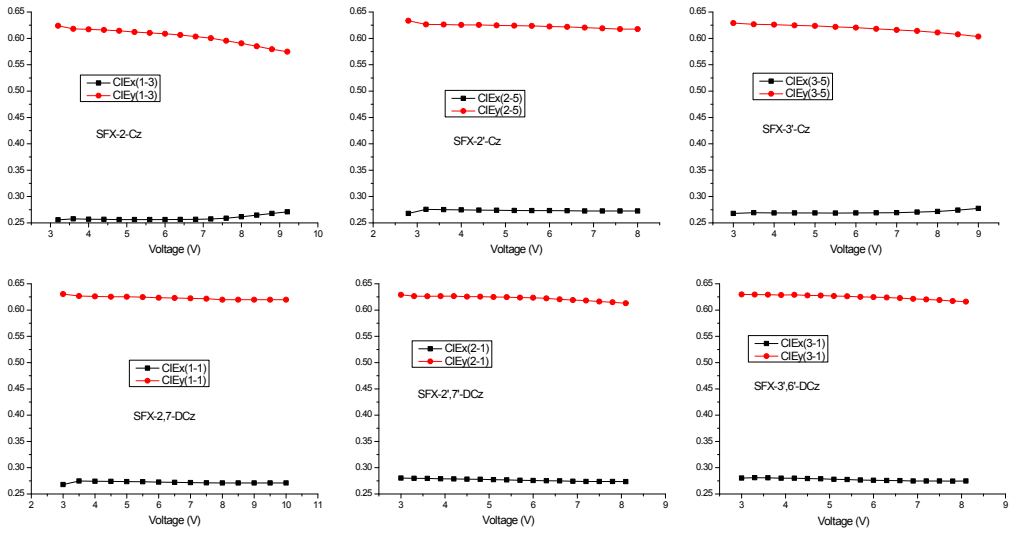

Figure S25. The CIE coordinates versus the voltage of the green devices based on SFX-Cz hosts.

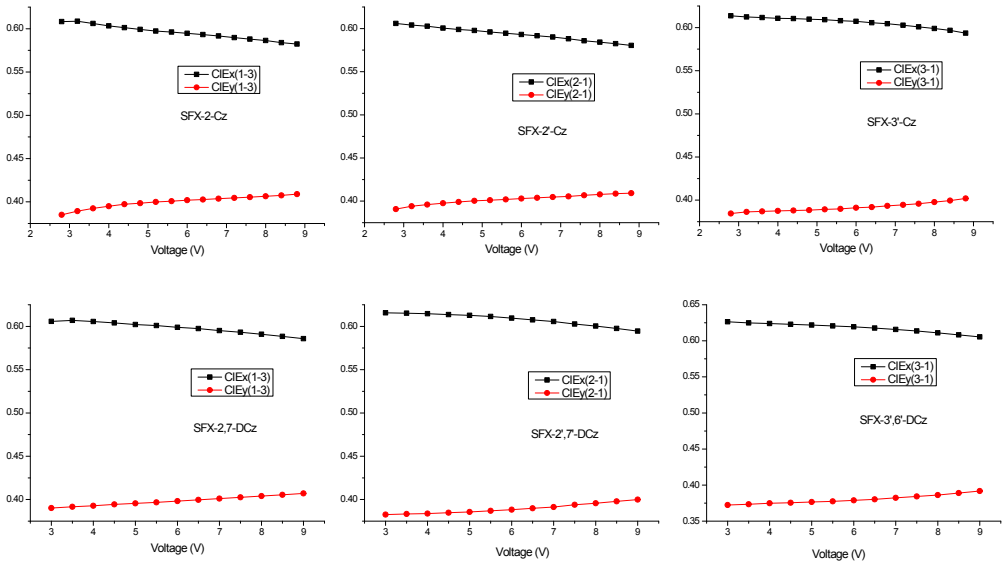

Figure S26. The CIE coordinates versus the voltage of the red devices based on SFX-Cz hosts.